POLITECNICO
MILANO 1863

SCUOLA DI INGEGNERIA INDUSTRIALE
E DELL'INFORMAZIONE

EXECUTIVE SUMMARY OF THE THESIS

Structure and properties of the polaron in doped poly(3-alkyl thiophenes): DFT modeling of the vibrational spectra.

TESI MAGISTRALE IN MATERIALS ENGINEERING AND NANOTECHNOLOGY – INGEGNERIA DEI MATERIALI E DELLE NANOTECNOLOGIE

AUTHOR: CARLO SAPORITI

ADVISOR: CHIARA CASTIGLIONI **CO-ADVISOR: DANIELE FAZZI**

ACADEMIC YEAR: 2022-2023

1. Introduction

π-conjugated polymers, and in particular, poly(3-hexyl thiophene) (P3HT), are organic functional materials of great interest for their peculiar chemical-physical and opto-electronic properties. Such class of materials is currently extensively investigated by the scientific community, both on a fundamental and applied research level, in order to pave the way for their technological applications as active materials for organic solar cells (OSCs), light emitting diodes (OLEDs) and field effect transistors (OFETs) **[1]**. Notably, some electronic applications, like the development of organic thermo-electric devices and chemical sensors, require an enhancement of the electrical conductivity of the material, a feature that can be obtained if the polymer is properly doped **[1,2].**

Doping induces changes in the molecular and electronic structure of the materials, determining for instance the variation of the vibrational nuclear dynamics, since the large π electrons-phonon coupling which characterizes the organic functional materials. For this reason, vibrational spectroscopy, namely IR and Raman spectroscopy, is a powerful characterization technique for the investigation of both structural and electronic properties **[3-6]**.

The main purpose of this Thesis is the application of Density Functional Theory (DFT) for the simulation of the spectroscopic response of P3HT and its oligomers in their neutral (pristine) and charged (doped) forms. DFT simulations allow obtaining insights, at the molecular level, of the doping induced charge defect, i.e. the so-called polaron, through its nuclear vibrations. Passing from the neutral to the charged (doped) state, the IR and Raman spectra of π-conjugated systems exhibit new intense bands in the 1000 and 1600 cm^{-1} wavenumber region. These bands are generally silent, or barely silent, in both IR and Raman spectra of the pristine state. For this reason, these doped-induced bands are called IRAVs (Infrared Activated Vibrations) and RAVs (Raman Activated Vibrations), and constitute the spectroscopic fingerprints of the charged species, namely the polaron.

A theoretical investigation of the structural and electronic features of the polaron is of fundamental importance to understand its physical properties,

like the charge transport features, aiming at the design of organic materials-based devices for the novel and sustainable opto-electronic applications.

2. Methods and models

Firstly, DFT based quantum-chemical calculations are applied to molecular models of isolated neutral and singly charged (i.e., radical cation) unsubstituted oligothiophenes, with an increasing number of thiophene rings (from six - T6, to fourteen - T14). These structural models are implemented to study the effect of the chain length on the frequency and intensity of the most relevant IR and Raman active normal modes. This strategy allows to understand which is the minimum chain length such that the spectroscopic features approach plateau values, and so to identify the most suitable molecular model to simulate the P3HT. Moreover, oligothiophenes with a sufficiently long chain allow to take into account for the self-localization of the polaron, and to evaluate its spatial extent (delocalization) in terms of number of thiophene units.

As a second step, to better simulate the experimental spectra of P3HT, more realistic structural models than the previous ones, namely oligothiophenes with alkyl lateral side chains, are introduced. As previously discussed, both neutral and charged species have been investigated. The exploited molecular models are the octamer of 3-hexyl thiophene (3HT8) and two ethyl-substituted oligothiophenes (3ET8 and 3ET12). They allow to study the effect of the lateral substituents on the spectroscopic and geometrical features. For the whole set of molecular models, the DFT simulations are carried out *in vacuo*, that is not taking into account any kind of intermolecular interactions with the surrounding environment (e.g., other polymer chains). Furthermore, for all the charged models, we do not consider for instance the presence of a dopant counterion as occurs in the experiments, since the systems are treated as isolated radical cations. DFT quantum-chemical calculations are performed with the Pople valence double-split 6-31G** basis sets with polarization and diffusion functions by adopting both the B3LYP and the range-separated CAM-B3LYP functionals. CAM-B3LYP is introduced to limit the Self Interaction Error (SIE) characterizing the DFT method. Indeed, SIE leads to an over-delocalization of the electronic structure, especially for charged states, a typical issue encountered by the B3LYP functional. All neutral molecular models, both the unsubstituted oligothiophenes and those with the lateral alkyl chains, are constrained to a planar backbone geometry. The planar backbone is inspired by the experimental solid-state molecular structure of P3HT. However, the planar structure is not the most energetically stable geometry when the molecules are treated *in vacuo*: if full geometry optimization of the oligothiophenes is performed, the backbone assumes a non-planar conformation. Similar considerations regard the oligothiophenes in their charged state. Among all the exploited molecular models, only the results regarding the unsubstituted and alkyl-substituted dodecamer will be considered in this summary.

3. Optimized geometries of neutral and charged oligothiophenes: relaxation upon charging and polaron size.

The charge injection into the oligothiophene upon the doping process induces a structural relaxation of the backbone, especially involving the quasi-single and quasi-double CC bonds. The analysis of the CC bond lengths of neutral and charged oligothiophenes, reported in Figure 1, allows estimating the polaron delocalization length. The perturbed region of T12 is identified by considering the variation of the bond lengths ($\Delta R_i = R_i^{charged} - R_i^{neutral}$) computed as the difference between the equilibrium length of the i-th bond in the charged state and the same bond in the neutral state. Quite arbitrarily, bonds belonging to the polaron are identified based on the criterion: $\Delta R \geq 0.5\ \Delta R^{max}$, where ΔR^{max} is the maximum bond length difference obtained, corresponding to the central CC bond. In Figure 1 both B3LYP and CAM-B3LYP results are reported. In the case of B3LYP the threshold value for ΔR is 0,01 Å, while in the case of CAM-B3LYP is 0,02 Å. In Figure 1 the symbol X (green for B3LYP case and yellow for CAM-B3LYP) is introduced to indicate the first and last CC bond, whose ΔR value reaches the threshold.

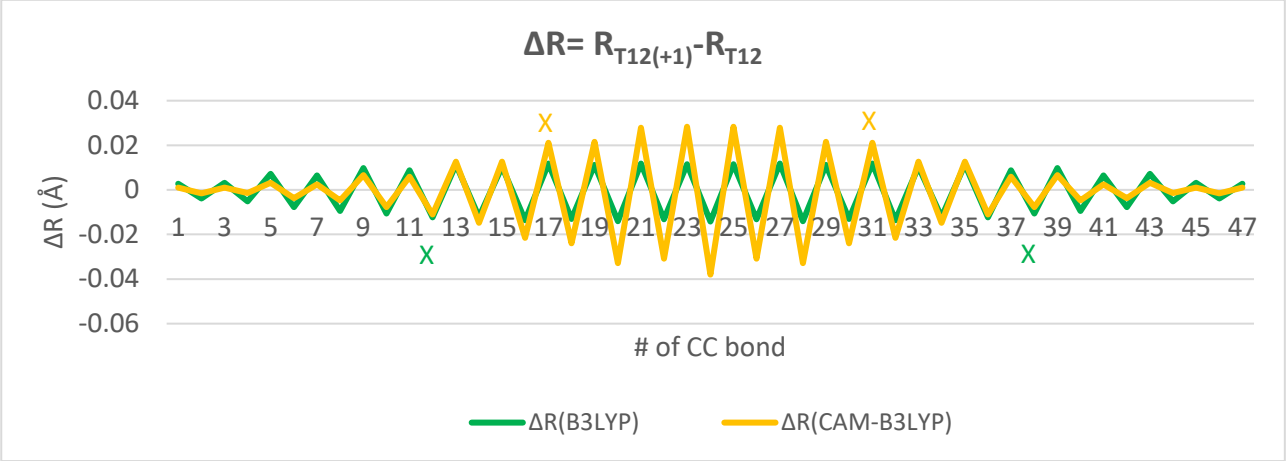

Figure 1: bond length difference (ΔR) between the CC bonds of the charged oligothiophene T12(+1) and the corresponding one of the neutral species T12. B3LYP (green line) and CAM-B3LP (yellow line) data. The CC bonds are numbered along the CC sequence forming the molecular backbone, from the left end to the right end of the molecule.

Figure 1 shows the spatial localization of the polaron as described by CAM-B3LYP, which confines the structural relaxation of the charged state in the central part of the oligomer chain. This is in net contrast with respect to B3LYP, which delocalizes the charge defect over a larger portion of the chain. The polaron delocalization length predicted by CAM-B3LYP and B3LYP are four and seven thiophene units, respectively. The analysis of the Bond Length Alternation (BLA) parameter, computed as the difference between the equilibrium length of each CC bond at even sites and the one of the adjacent CC bond (odd sites), allows to rationalize the structure relaxation following the polaron formation. Figures 2 and 3 report the values of the BLA of T12 and T12(+1), as predicted by B3LYP and CAM-B3LYP respectively.

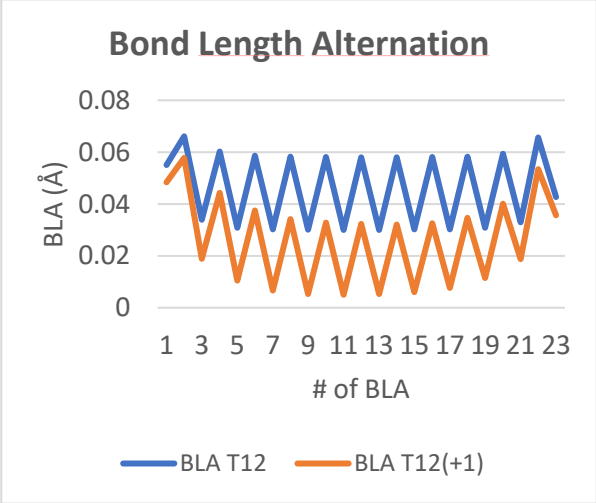

Figure 2: B3LYP-calculated Bond Length Alternation (BLA) of neutral (blue) and charged (orange) T12.

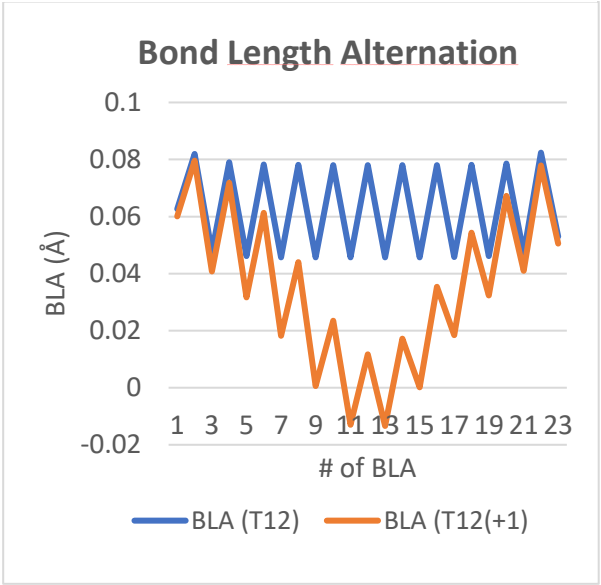

Figure 3: CAM-B3LYP-calculated Bond Length Alternation (BLA) of neutral (blue) and charged (orange) T12.

Figures 2 and 3 show that:

1) BLA of neutral T12 is positive and quite large: the pristine oligothiophenes are conjugated materials, with a backbone characterized by alternated quasi-single and quasi-double CC bonds.
2) BLA of the neutral oligomers and that of the corresponding charged species are very similar for the CC bonds close to the terminals, thus confirming that the polaron self-localizes in the central region of the molecule, while the peripheral

thiophene units remain unaltered upon the doping process.

3) BLA calculated with CAM-B3LYP functional exhibit small but negative values in the central region of the molecule, thus meaning that the most perturbed CC bonds by the charge injection invert their character of quasi-single and quasi-double bonds. According to the description provided by CAM-B3LYP, the region perturbed by the charge exhibits a remarkably relaxed geometry with a quinoid feature. This is the main difference with the prediction obtained at the B3LYP level, which shows equalized quasi-single and quasi-double CC bonds.

CAM-B3LYP provides structural relaxations and a delocalization length of the polaronic species closer to the experimental findings than B3LYP. On the contrary, the calculation of the vibrational spectra of the charged models (not discussed here), presents several issues when carried out at the CAM-B3LYP level, while it provides quite reliable results at the B3LYP level. In the attempt to overcome these problems, a hybrid approach, that combines the positive performances of the two different functionals, is introduced, leading to a two-step method: at first, a geometry *optimization* performed with CAM-B3LYP, second, a frequency and intensity calculations (on top of CAM-B3LYP geometries) at the B3LYP level.

4. Prediction of the Vibrational spectra: IRAV and RAV as polarons signature.

The DFT calculation of the vibrational spectra for the whole set of neutral and charged unsubstituted oligothiophenes and for the alkyl-substituted oligothiophenes, in their neutral and charged state, was performed. On this ground, a careful investigation on size-confinement effects on the IR and Raman features is carried out. For sake of conciseness, in the following we will illustrate the results obtained for a few selected models.

4.1. Prediction of the IR and Raman Spectra of neutral and charged P3HT oligomers.

Figure 4 reports the IR (top panel) and Raman spectra (bottom panel) of neutral T12 (blue lines) and charged T12(+1) (orange lines) in the wavenumber region between 1000 and 1600 cm^{-1}, as predicted with B3LYP (solid lines) and with the hybrid approach (CAM-B3LYP//B3LYP) (dashed lines).

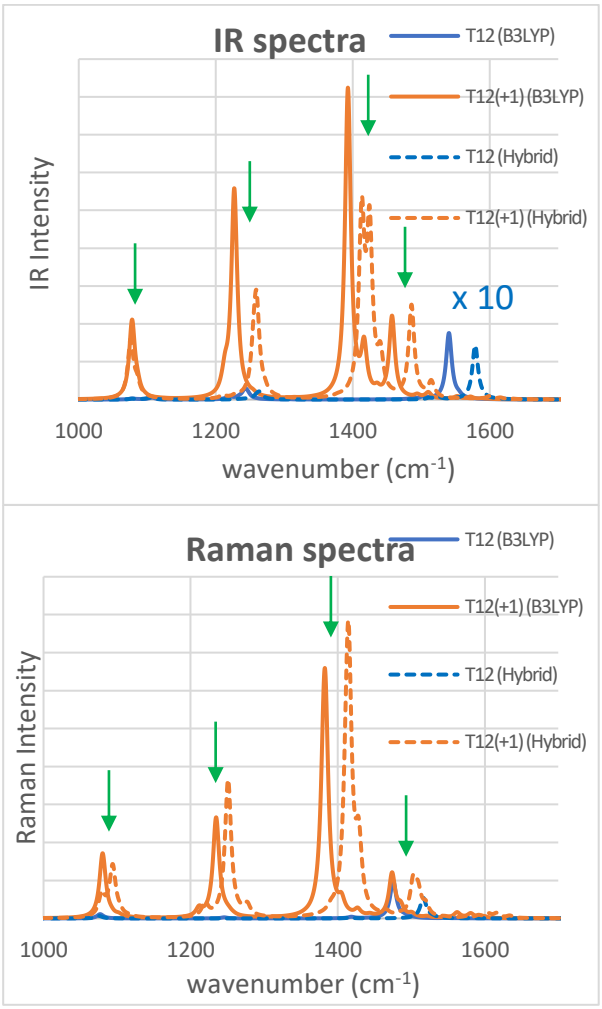

Figure 4: IR (top panel) and Raman spectra (bottom panel) of neutral T12 (blue lines) and charged T12(+1) (orange lines), predicted by B3LYP (solid lines) and with the hybrid approach (dashed lines).

IR and Raman spectra of T12(+1) are characterized by four intense peaks (see green arrows), which are silent or barely silent in the IR and almost inactive in the Raman when the oligothiophene is in the neutral state. Indeed, DFT simulations of charged species show the appearance in the IR and Raman spectra of the so-called IRAVs and RAVs, which

constitute the vibrational spectroscopic fingerprints of the polaron. The four IRAVs and RAVs peaks pattern is equally computed by both the B3LYP and hybrid approach. The latter predicts the active peaks at a higher frequency than B3LYP, a feature due to the larger BLA as computed with CAM-B3LYP.

4.2. Local intensity parameters; IRAVs and RAVs activation mechanisms.

The analysis of the IR local parameters, namely the dipole derivative with respect to the internal CC bond stretching coordinate (∂**M**/∂R), and of the eigenvectors of the normal modes associated to the IRAVs allows the full rationalization of their activation mechanisms. Moreover, they explain the very high intensity of the IRAVs upon doping (i.e., a full electron transfer process). In particular, for the case of charged oligothiophenes, the parameter $\partial M_y/\partial R$ (y coincides with the chain axis) exhibits a systematic alternation of positive and negative values. This behaviour explains the onset of the IRAVs upon doping. In fact, IRAV bands are assigned to ECC-like normal modes, that are characterized by an alternating stretching and shrinking of the subsequent C-C bonds along the backbone, as revealed by the analysis of the vibrational eigenvectors. This alternate bond stretching and shrinking of the ECC-like vibrations is coherent with the pattern displayed by the $\partial M_y/\partial R$ parameters, thus resulting in net positive contributions leading to high IR intensities. Moreover, the values of $\partial \mathbf{M}_y/\partial R$ for charged oligothiophenes are very high with respect to those of neutral oligomers, thus explaining the huge intensity of the IRAVs.

The activation mechanism of ECC-like IRAVs can be better rationalized through the explicit definition of the Effective Conjugation Coordinate (ECC) for a general oligothiophene. Figure 5 reports the numbering of the CC bonds, used to properly define the ECC coordinate (also called Я), for a prototypical T2 unit **[4]**.

$$Я = \frac{1}{\sqrt{8}}(R_2 - R_1 + R_4 - R_3 + R_6 - R_5 + R_8 - R_7) \quad (1)$$

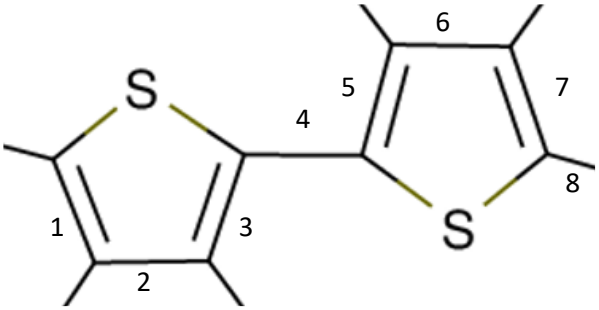

Figure 5: CC bond numbering for a bithiophene unit.

Eq. 1 can be easily extended to any oligomer formed by an even number of thiophene units.

The expression of the dipole derivative with respect to a normal mode Q_k is:

$$\frac{\partial M_y}{\partial Q_k} = \sum_t \frac{\partial M_y}{\partial r_t} L_{tk} \cong \sum_i \frac{\partial M_y}{\partial R_i} L_{ik} \quad (2)$$

where Q_k is the k-th normal coordinate, $\{r_t\}$ is the set of the internal valence coordinates, L_{tk} is the element of the vibrational eigenvector expressed on the basis set of the internal coordinates, $\{R_i\}$ is the sub-set of the C-C stretching internal coordinates **[4,5]**. The approximated equality holds for normal modes such as ECC-like vibrations of the doped molecules, because the dipole derivatives with respect to the CC stretching internal coordinates have remarkably high values compared to the other dipole derivatives.

In the case of charged oligothiophenes $\frac{\partial M_y}{\partial R_i}$ presents opposite sign for the stretching of adjacent CC bonds and also L_{ik} associated to an ECC-like mode have opposite sign too, for a quasi-single (even sites) or a quasi-double CC (odd sites) bond (eq. 1). For the above reasons, the contributions from the individual CC bonds to $\frac{\partial M_y}{\partial Q_k}$ sum up, thus explaining the very high IR intensity of the ECC-like normal mode. Importantly, the strongest IRAV is an ECC-like mode with one node on the central CC bond (ungerade symmetry): the L_{ik} elements exactly follow the systematic change in sign of the $\frac{\partial M_y}{\partial R_i}$ parameters while crossing the central bond.

Analogue considerations are valid for the simulated RAVs, which are fully rationalized by means of the Raman local parameters, namely the polarizability derivative with respect to the internal CC bond stretching coordinate (∂**α**/∂R). Indeed, the strongest RAVs exhibit a coherent

stretching and shrinking pattern with the one of the $\partial\boldsymbol{\alpha}/\partial R$ parameters. The absolute values of $\partial\alpha/\partial R$ parameters of T12(+1) are much larger with respect to the ones showed by the corresponding neutral oligomer, thus explaining the dramatic increasing of the intensity of the Raman spectrum and in particular of the extremely high Raman activity of the normal modes showing ECC-like character. The rationalization of this aspect can be obtained through the definition of the polarizability derivative with respect to the C-C stretching internal coordinate, according to the following equation **[4]**:

$$\frac{\partial \boldsymbol{\alpha}}{\partial Q_k} = \sum_t \frac{\partial \alpha}{\partial r_t} L_{tk} \cong \sum_i \frac{\partial \alpha}{\partial R_i} L_{ik} \qquad (3)$$

Based on the definition of the Я coordinate, quasi-single and quasi-double CC bonds stretch out-of-phase in ECC-like normal modes and so L_{tk} presents values with opposite sign; also $\frac{\partial \boldsymbol{\alpha}}{\partial R_i}$ shows positive and negative values and so the contributions from the individual CC bonds to $\frac{\partial \boldsymbol{\alpha}}{\partial Q_k}$ sum up, implying very large Raman activity of the ECC-like normal modes.

Above considerations are illustrated in Figures 6 and 7, which show the IR and Raman local parameters and the sketch of the eigenvector of the normal mode of the most intense IRAV and RAV, respectively. Notably, the strongest RAV is an ECC-like mode with two nodes: the L_{ik} elements exactly follow the systematic change in sign of the $\frac{\partial \boldsymbol{\alpha}}{\partial R_i}$ parameters while crossing the polaron region.

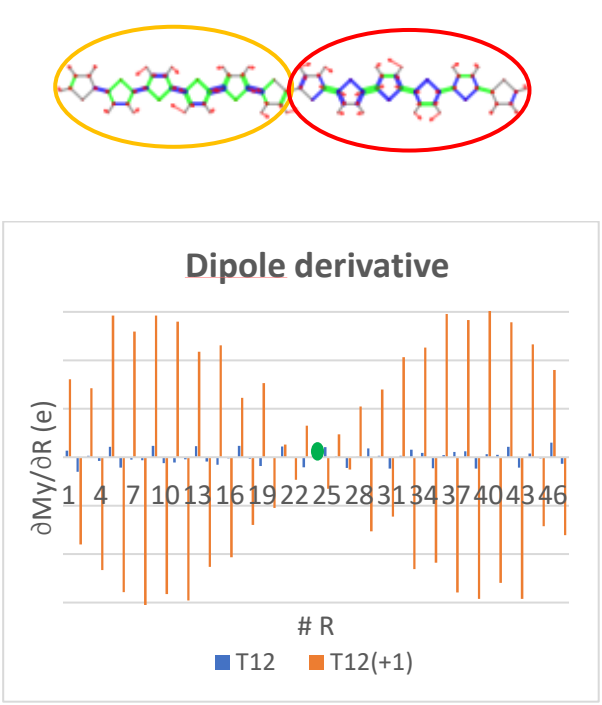

Figure 6: top panel: sketch of the eigenvector of the normal mode of the most intense IRAV of T12(+1). Bottom panel: IR local parameters of neutral T12 and charged T12(+1).

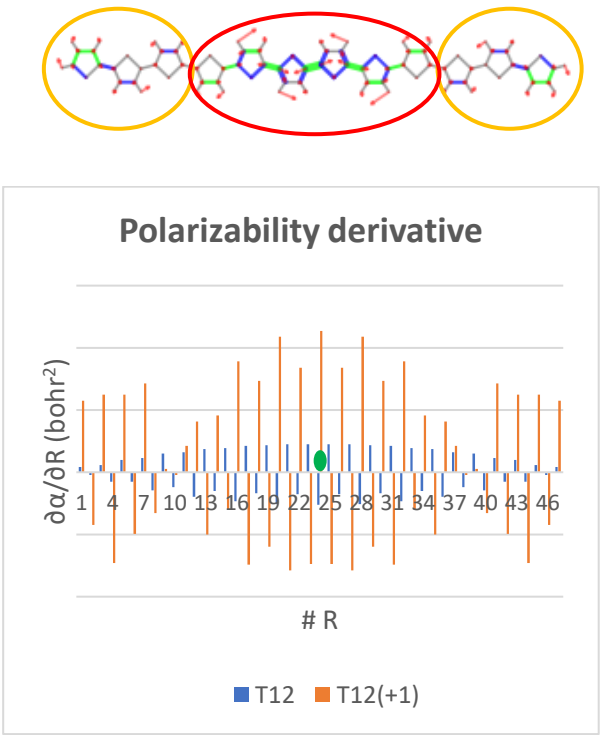

Figure 7: top panel: sketch of the eigenvector of the normal mode of the most intense RAV of T12(+1). Bottom panel: Raman local parameters ($\frac{\partial \boldsymbol{\alpha}}{\partial R_i}$ = trace ($\frac{\partial \boldsymbol{\alpha}}{\partial R_i}$)) of neutral T12 and charged T12(+1).

DFT calculations of alkyl-substituted oligothiophenes present analogue results if compared to those of the unsubstituted oligomers. In particular, IRAVs and RAVs patterns are barely affected by the presence of the lateral alkyl chains, even though the substituted oligomers are characterized by a higher number of active vibrations due to the dynamic coupling of the alkyl chains with the molecular backbone. Importantly, the IRAVs and RAVs activation mechanisms are the same described for the unsubstituted oligothiophenes, thus meaning that the occurrence of these features does not depend on the symmetry of the system but on the electronic charged state, resulting from the full hole transfer from the dopant to the oligothiophene. As a further proof, the same conclusion can be obtained even substituting the lateral alkyl chains from hexyl to ethyl. These results demonstrate that the IRAVs and RAVs represent the IR and Raman spectroscopic fingerprints of the polaron, regardless the molecular model adopted.

5. Comparison between DFT simulations and experiments: IR and Raman spectra of doped P3HT.

Figures 8 and 9 report a comparison between the experimental IR and Raman spectra of I_2-doped P3HT (chemical doping procedure) with the DFT spectra computed with B3LYP and the hybrid-approach (CAM-B3LYP//B3LYP), for the charged 3-ethyl-dodecamer 3ET12(+1). The theoretical spectra are scaled by a factor of 0,9742.

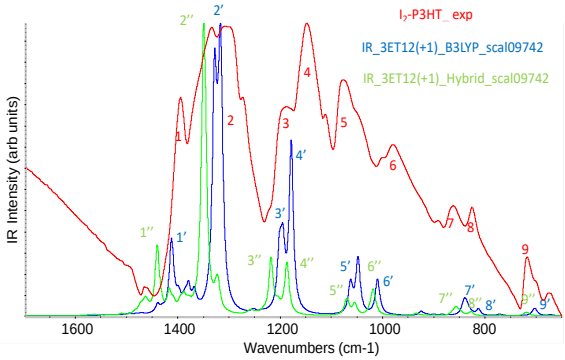

Figure 8: B3LYP and hybrid (CAM-B3LYP//B3LYP) approach IR spectra of the dodecamer of 3-ethyl thiophene and the experimental spectrum of chemically doped (I2 dopant) P3HT.

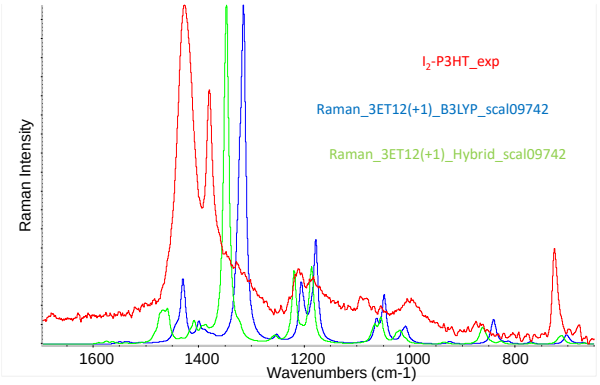

Figure 9: B3LYP and hybrid (CAM-B3LYP//B3LYP) approach Raman spectra of the dodecamer of 3-ethyl thiophene and the experimental spectrum of chemically doped (I2 dopant) P3HT.

Figure 8 shows that the simulated spectrum of 3ET12(+1) is in good agreement with the experimental results. The IRAVs pattern is properly predicted by the DFT simulations, thus corroborating the experimental results. On the contrary, Figure 9 shows that the simulated Raman spectra feature the most intense RAV peak with a very high intensity and low frequency, such that it does not find correspondence with the main peaks observed in the experimental Raman spectrum of chemically doped P3HT. The latter are indeed slightly red-shifted with respect to those of the pristine, neutral polymer. These results show that a reliable DFT simulation of the Raman spectrum of charged species is very challenging and other simulation strategies (to mention few, for instance, the inclusion of resonance effects by considering electronically excited states, the inclusion of explicit dopant(s), the inclusion of explicit intermolecular interactions, a better description of correlation and multi-determinant effects, etc.) should be considered in order to reproduce the experimental data.

6. Conclusion

DFT simulations correctly predict the vibrational spectra of the neutral (pristine) species and the IRAVs of the charged (doped) oligothiophenes, allowing for their complete rationalization through the joint study of the local IR intensity parameters and the analysis of the ECC-like normal mode eigenvectors. Moreover, the study of the structural relaxation occurring upon doping allows for the estimation of the polaron delocalization length. On the contrary, the DFT calculation of the Raman

spectra of charged species (RAVs) is very complicated: according to a very preliminary test, we found that models able to explicitly take into account the intermolecular interactions between the oligothiophene and the dopant counterion are able to simulate reasonably well the Raman spectrum. This finding opens the way to new approaches for the quantum-chemical description of the vibrational spectroscopic response of doped π-conjugated materials, which represents a tremendous challenge in the field of molecular and materials modelling.

7. Bibliography

[1] Skotheim, T. A., (ed.). Handbook of Conducting Polymers, (Dekker, New York), 1986.

[2] Zou, Y.; Di, C.A.; Zhu, D. Chemical Doping of Organic Semiconductors for Thermoelectric Applications. Chem. Soc. Rev. 2020, 49, 7210–7228.

[3] Yin, J.; Wang, Z.; Fazzi, D.; Shen, Z.; Soci, C. First-Principles Study of the Nuclear Dynamics of doped conjugated Polymers. J. Phys. Chem. C 2016, 120, 1994-2001.

[4] Gussoni, M.; Castiglioni, C.; Zerbi, G. Vibrational spectroscopy of polyconjugated materials: polyacetylene and polyenes. In Clark R J J, Hester R E (eds.), Spectroscopy of advanced materials, (Wiley, New York) 1991, Ch 5, 251-353.

[5] Castiglioni, C.; Tommasini, M. Infrared Active Vibrations in Doped π-Conjugated Materials: The Mechanism of Activation of Raman Modes. Asian J. Phys. 2022, 31, 14221–1776.

[6] Castiglioni, C.; Tommasini, M.; Zerbi, G. Raman Spectroscopy of Polyconjugated Molecules and Materials: Confinement Effect in One and Two Dimensions, Philos Trans R Soc A 2004, 362, 2425–2459.